

<input type="checkbox"/>	序号	排序码	项目编号	项目名称	项目类型	项目级别	学科门类	专业类	第一主持人	第一主持人所属学院	第一指导教师
<input type="checkbox"/>	1	7	2023105641154	磷酸锰铁锂正极材料及其全固态电池的制备与性能探究 学生申报	创新训练项目	校级	理学	化学类	黄潼欣 202133210114	材料与能源学院	庄慧 30004986
<input type="checkbox"/>	2	7	2024105641009	杂原子掺杂二氧化钛微球的制备及其储钠性能研究 学生申报	创新训练项目	校级	理学	化学类	黄文希 202233210108	材料与能源学院	庄慧 30004986

证书编号: GD000024855625



广东省专业技术人员继续教育证书

庄慧(身份证号: 430611199412205524) 参加
专业技术人员继续教育学习, 经审核, 已完成2024年度
实验技术 专业系列专业技
术人员继续教育学习任务, 根据《广东省专业技术人员
继续教育条例》, 特发此证。

发证单位:

发证时间: 2025年04月27日



广东省人力资源和社会保障厅制

说明: 证书可凭编号在广东省人力资源和社会保障厅门户网站核实

中国教育技术装备

China Educational Technology & Equipment

主管:中华人民共和国教育部 主办:中国教育装备行业协会 2024年第18期(9月下) 总第588期



理论研究

基于同伴互评的在线学习评价机制设计研究

信息技术

具身之美, 虚拟之术

装备应用

面向智能交通实践课程的微缩智能车设计方案及教学应用研究

装备建设

面向自动化类的工业互联网与数字孪生技术实训平台构建

ISSN 1671-489X



9 771671 489241

18>





1987年创刊（半月刊）

2024年9月下 第18期 总第588期

主管单位：中华人民共和国教育部

主办单位：中国教育装备行业协会

编辑出版：《中国教育技术装备》杂志社

顾问：王 富 李兴植

主编：朱俊英

常务副主编：王海明

副主编：赵晓宁

责任编辑：杨永坤 姜火明 马 赫

王 赢 宋利云

网址：<http://www.cete1987.com>

地址：北京市海淀区文慧园北路10号中教仪

办公楼5层 邮编：100088

投稿邮箱：cete1987@vip.163.com

编辑部电话：010-62112678（稿件查询）

广告、发行负责人及电话：甘甜 010-59893286

邮发代号：82-975

国内发行：中国邮政集团有限公司北京市报刊

发行局

国内订阅：中国邮政集团有限公司

国际标准连续出版物号：ISSN 1671-489X

国内统一连续出版物号：CN 11-4754/T

印刷：廊坊市瀚源印刷有限公司

国内定价：16元/期（RMB）

出版日期：每月15日、28日

版权所有 翻印必究



目次

CONTENTS

「特稿」

- 1 开封大学深化教育教学改革 新质生产力助推高质量发展
——访中国教育装备行业协会副会长、开封大学校长王德如研究员

「理论研究」

- 5 基于同伴互评的在线学习评价机制设计研究 赵凤梅 胡勇
14 新时期高职院校退役复学大学生再适应问题研究
薛国梁 贾东良
17 教育数字化视域下老年开放大学办学模式研究
张震 蔡大鹏 董黎明 艾海明

「教师发展」

- 22 高校辅导员就业指导服务能力测评与提升研究
彭晗 陈一柯 汪倩玉

「信息技术」

- 25 具身之美 虚拟之术
——关于智慧美育新路径的探索与思考
张欣茹 胡凡刚 逢仁霞

「装备应用」

- 29 基于创新人才培养的生命科学实验教学平台应用研究
郭宾会 杜坤
32 面向智能交通实践课程的微缩智能车设计方案及教学应用研究
李海舰 赵晓华 程俊 王威杰

「装备管理」

- 38 基于材料类专业研究生能力培养的大型仪器设备开放管理探索
郭敏娜 吕珺 汪冬梅 咎祥 黄露露
41 高校实验室安全现状与安全文化体系建设研究
邹佳鹏 范淑媛 刘辉

「装备建设」

- 45 面向自动化类的工业互联网与数字孪生技术实训平台构建
许继平 李卉 李佳乐 王昭洋 孔德政
50 三相交流异步电动机控制及故障诊断虚拟仿真实验系统设计与应用
王玲 张浩 朱书慧 叶卫东

「教学改革」

《中国教育技术装备》编辑委员会

编委会主任：靳 诺

编委会副主任：李 瀛 朱俊英

委员(以姓氏笔画为序)

- 马晓峰 全国工商联书业商会会长
王 戈 天津市教育科学研究院教育技术装备中心副主任
王 强 中国教育装备行业协会副会长
王 延 东北师范大学党委副书记
王会军 浙江省教育技术中心主任
王国强 四川省学校国有资产与教育装备中心主任
王海明 《中国教育技术装备》杂志社常务副主编
王新艳 山西省教育厅资助与保障中心主任
王德如 开封大学校长
卢 卫 广西壮族自治区教育技术和信息化中心副主任
闫明圣 安徽省电化教育馆馆长
任萍萍 科大讯飞股份有限公司集团副总裁
任雪松 辽宁教育学院教育装备研究与发展中心主任
朱玉荣 安徽文香信息技术有限公司董事长
朱圣芳 湖北省教育技术装备处处长
朱俊英 《中国教育技术装备》杂志社社长、主编
刘忠民 吉林省教育技术装备中心主任
刘殿房 河北沧狮文化体育科技发展有限公司董事长
孙庆文 新疆建设兵团教育技术装备管理中心主任
孙家栋 河南省教育资源保障中心主任
杨 湛 宁夏回族自治区教育装备和校园风险管理中心副主任
杨志军 云南省教育厅教学仪器装备中心主任
李 瀛 中国教育装备行业协会秘书长



- 中国学术期刊综合评价数据库来源期刊
- 中国基础教育知识仓库全文收录期刊
- 中国期刊全文数据库收录期刊
- 中文科技期刊数据库(全文版)收录期刊
- 中国核心期刊(遴选)数据库收录期刊
- 龙源期刊网收录期刊
- 本刊已进入IDF国际学术论文注册及服务序列,全部论文均具唯一DOI编码

目次

- 55 基于 OMO 的高校 IT 类课程教学改革探索与实践
——以 MySQL 数据库应用课程为例
董国钢 朱华 黄金 李广生
- 60 基于 SU 软件的道桥工程 CAD 双课双线一体化教学模式研究
卜政滔 李讯 陶礴
- 64 5E 教学模式应用于设备测试课程探索与实践
董海迪 金凯 袁胜智 李敏 李静
- 67 城市数字治理创新班人工智能概论课程实践 金苍宏 罗荣良
- 71 基于 OBE 理念的 C 语言程序设计思政育人研究与实践
高月芳 王栋 李玉峰 殷建军 黄玲
- 75 职业教育新型活页式教材的内涵特征和开发路径 杨杨
- 80 机电一体化系统设计课程思政教学改革初探
夏英凯 龙长江 吕许俊 陈红
- 83 虚实一体化的传感器技术及应用课程项目式教学实践
刘娇月 杨聚庆 喻武龙 祝家东 黄飞东
- 88 工程教育认证背景下高频电路课程改革与实践
聂秋玉 贺付亮 常飞

「教育技术」

- 92 SPOC 混合式教学模式实践应用
——以防灾减灾工程课程教学为例
孙茂好 刘婷婷 李己华
- 97 面向新管科人才培养的运筹学课程混合式教学模式构建研究
董书琴 刘小虎 张玉臣 汪永伟 吴疆
- 102 数字化教育背景下多维混合式教学模式探索与实践
——以 DSP 技术课程为例
李栋 高志奇 张占强 王艳荣 董亦凡 曹琪
- 106 智慧教学背景下混合式教学模式探究
——以精细化学品复配原理及配方设计课程为例
王晓红 付凤艳 高志华

- 110 项目驱动混合式教学模式在工程力学课程中的探索与实践
梁艳 赵小健 程芳 龙永东

「科学教育」

- 114 面向 4C 能力培养的创客教育教学模式设计 张玮 顾倩颐

「实验教学」

- 120 大学物理实验课程思政建设研究与探索 侯宏涛

CONTENTS

- 126 虚实融合三位一体的数字电路与逻辑设计实验教学模式创新
田慕玲 王跃龙 李春叶
- 132 基于 HALCON 的机器视觉识别综合实验项目设计
茅靖峰 丁寅佳 李奔 徐一鸣
- 138 以高分子为试剂的有机化学实验教学探索
王明存 王红山 陈贻焱
- 142 新工科背景下消防工程专业实验教学改革探讨
——以河南理工大学消防工程专业为例
裴蓓 胡紫维 潘荣锟 张学博 李波
- 146 双一流建设背景下物理化学实验课程思政探索
庄慧

「实践实训」

- 149 测量综合实习课程思政实践与思考
余建杰 曹志 刘碧霞
- 153 新工科建设背景下无人驾驶开放创新实践教学模式研究
柴锦 张庆 吴涛 李东轶
- 156 基于职业发展导向的高职院校学生能力素质培养路径研究
杨赞 汤卫

「实践育人」

- 161 新工科引领的微电子专业实践创新型人才培养模式探索
彭木 黄凤兰
- 165 新技术对新疆北部中职教育的影响分析
——以阿勒泰地区中职教育为例 赵倩 郑立云 林闽智
- 168 欢迎订阅《中国教育技术装备》

广告

封2: 织里校服
封3: 东泰教育
封底: 国庆公益广告
彩插: 未力科技

- 李有增 中国教育装备行业协会副会长
何光辉 福建省教育装备与基建中心主任
沈本领 江苏省教育装备与勤工俭学管理中心主任
宋东茂 北京中庆现代技术股份有限公司董事长
陈京 河北省教育技术中心主任
陈瑜 重庆市教育信息技术与装备中心主任
陈登贵 广东广视通科教设备有限公司董事长
张万敏 湖南省教育生产装备处处长
张宇生 立达信物联科技股份有限公司副总裁
张红星 内蒙古自治区教育装备技术中心主任
张泽均 重庆汇聚教学设备有限公司董事长
张建锋 广东省教育装备中心主任
张树江 鸿合科技股份有限公司副董事长
张惠敏 深圳市教育信息技术中心主任
武装 北京市数字教育中心主任
季琳琦 上海东方教具有限公司总经理
竺建伟 上海教育装备行业协会会长
单泓水 新疆维吾尔自治区教育技术与资源发展中心党总支书记
赵梦 陕西省教育装备行业协会会长
施建国 中国教育装备行业协会教育装备研究院副院长
秦志功 甘肃省教育装备办公室主任
袁振国 华东师范大学教授、博士生导师
夏越 教育部宣传教育中心副主任
夏国明 中国教育装备行业协会副会长
顾建军 南京师范大学教授、博士生导师
徐涛 上海市教育委员会教育技术装备中心主任
郭颢 黑龙江教师发展学院教育信息化研培与传媒中心(黑龙江省电化教育馆)主任
唐林伟 浙江师范大学现代职业教育研究院院长
黄荣怀 北京师范大学教授、博士生导师
董恩 陕西省教育厅教育技术装备管理中心主任
靳诺 中国教育装备行业协会会长
魏光祥 山东省教育发展服务中心主任

本刊声明

- 未经本刊许可,不得转载、摘编本刊所刊载文章。
- 作者如不同意文章被本刊合作网站收录,请提前告知本刊。
- 本刊所载文章观点不代表本刊立场,作者文责自负。
- 本刊从未委托任何个人或机构代为征稿,凡投本刊稿件,请通过腾云采编系统(<http://zjyb.cbpt.cnki.net>)投稿。
- 凡投本刊稿件,投稿30天内未接到反馈信息,可另行处理。
- 作者请勿抄袭,请勿一稿多投。



双一流建设背景下物理化学实验课程思政探索

庄慧

华南农业大学基础实验与实践训练中心 广州 510630

摘要 开展课程思政是“双一流”建设背景下理工科专业实验教学的必经之路^[1]。在“双一流”建设背景下开展课程思政,可以有效增强物理化学实验教学效果。以华南农业大学为例,介绍其基础实验与实践训练中心在物理化学实验教学中融合专业知识和思政教育的探索,以期在教学过程中实现智育与德育相统一^[2],落实立德树人根本任务,同时为其他理工科专业的实验教学课程思政建设提供参考与借鉴。

关键词 双一流; 物理化学实验; 课程思政; 立德树人

中图分类号: G642.423 **文献标识码**: B

文章编号: 1671-489X(2024)18-0146-03

0 引言

“双一流”建设即建设世界一流大学和世界一流学科,是我国在新的历史时期为整体提升人才培养水平、增强我国在国际上的核心竞争力和未来发展的驱动力作出的重要决策。在2016年12月召开的全国高校思想政治工作会议上,习近平总书记强调:要坚持把立德树人作为中心环节,把思想政治工作贯穿教育教学全过程,实现全程育人、全方位育人,努力开创我国高等教育事业发展新局面^[3]。华南农业大学是一所以农立校的综合性大学,始终将立德树人作为立校之本,着力培养适应时代发展、担当民族复兴大任的高素质人才,并于2022年入选国家“双一流”建设高校。将课程思政理念融入课程教学,是在“双一流”建设背景下高校把握教育改革发展的正确方向、提升教师教书育人水平、提高人才培养质量的制胜一招。

物理化学实验课程包括物理化学实验基本知识、热力学、动力学、电化学、表面化学和胶体化学等相关内容,兼具科学性和实用性。物理化学涉及的概念较为抽象,常常涉及复杂的数学运算和推导,对实验操作技巧要求较高。且物理化学作为一门综合性学科,知识面广、深度大,对教师教学和学生学

习都提出挑战。这导致一些教师在授课过程中偏向于讲解理论原理、仪器设备的操作和数据的分析处理等方面,而忽视学生的思想政治教育。基

1 构建物理化学实验课程思政体系

思政教育与物理化学实验课程教学应该以何种方式结合起来,目前还缺少适配的指导体系。因此,需要对课程思政建设进行统筹规划,对物理化学实验课程思政育人目标进行挖掘和细化,不断探究和拓展实施课程思政建设的途径,挖掘出色、典型的思政建设案例,达到春风化雨、润物无声的育人效果。

1.1 组建实验课程思政教学团队

各学院和中心要出台相关政策和制度,积极鼓励、引导物理化学实验任课教师与中心实验技术人员加入课程思政队伍,并吸纳专业思政课程教师,由此形成物理化学实验课程思政教学团队,确保课程思政工作的顺利开展和持续深化。团队教师不仅需要具备扎实的学术素养和教学水平,更需要具备较高的思政能力和素养。因此,团队成员需要不断提升思政理论水平,加强对国家政策、社会热点和时事问题的学习和了解,以更好地进行课程思政教学。此外,还需要加强团队协作和沟通,促进教师之间的交流与合作。团队成员可以通过共同备课、定期研讨、交流经验等方式相互学习、相互借鉴,不断提升教学水平和思政水平^[4]。

1.2 完善实验教学大纲

首先,审视实验教学大纲的编写,将课程目标明确为不只是传授知识和技能,更要培养学生的思想品德和社会责任感。其次,针对物理化学实验的特点和目的,对实验内容、方法、要求等进行细致梳理和精心设计。在此过程中,注重强调实验过程中的安全意识、团队合作精神、科学严谨性等方面,培养学生的品德修养和社会责任感。同时,将课程内容与时事热点、社会问题相结合,引导学生思考

作者简介:庄慧,助理实验师。

科学技术与社会发展的关系,激发学生的社会责任感和创新意识。经过专业思政教师的指导,通过集体备课、优化教学案例等方法,不断完善教学大纲,探索课程思政在物理化学实验课中的实施形式和方法^[5]。

1.3 运用合适的教学方法与手段

在课程思政开展过程中应注重灵活运用恰当的教学方法与手段。教师应注重以学生为本,并根据物理化学实验教学内容与时俱进地完善与优化实验教学方法,例如:可以采用启发式教学法,通过设计具有启发性的实验操作和问题,引导学生主动探索、发现知识;可以利用案例教学法,引入生动的案例和实践情境,让学生在实验中感受科学知识与社会现实的联系,培养学生的社会责任感和实践能力;还可以采用小组讨论、角色扮演、反思性讨论等多种教学方法,增强学生的思辨能力和创新意识,引导学生深入思考并形成独立见解。

随着信息技术的发展,许多先进的教学手段应运而生,如慕课、微课、虚拟仿真教学等,这些教学手段提供了更加便捷和灵活的学习途径,满足了学生个性化的学习需求,有利于学生产生情感共鸣,进而增强课程思政效果。中心搭建了线上实验教学平台,旨在为学生提供更为便捷、灵活的学习环境以及丰富的学习资源和支持。学生还可以将每次实验课后的心得体会上传至平台,便于教师根据学生的心得体会及时了解学生在物理化学实验学习中的思想动态,不断优化课程思政的实施策略,提高思政教育工作的针对性和科学化水平,进一步促进课程思政目标的实现。

1.4 建立健全评价机制

首先,重新审视现有的评价指标和权重分配,将德育考核纳入其中。增加对学生思想品德、社会责任感、团队合作精神等方面的评价指标,并适当提高其在评价体系中的权重,在平时表现、实验报告和期末考试中增加对学生思政素养的评价内容。例如:可以针对实验报告中学生对科学道德、社会影响、环境保护等方面的思考和表达,以及在实验操作和课堂讨论中展现出的团队合作、沟通交流等能力进行评价;还可以在课堂教学中引入相关的案例分析和思政教育话题,通过讨论和互动的方式引导学生思考并表达自己的观点。通过这些讨论和案例分析,评价学生的思想品德和社会责任感。

其次,建立学生与教师之间的双向反馈机制,鼓励学生提出对思政教育的反馈意见和建议,同时教师也应及时关注学生的思想动态和学习状态,做好个性化的辅导和指导工作。

最后,综合运用定性和定量评价方法,对学生

的思政素养进行全面评估。

通过以上措施,可以在现有的教学评价体系中有效地融入对学生的思政考核,全面推进物理化学实验课程思政建设,增强教学效果^[6]。

2 挖掘思政映射与融入点

课程思政不是将课程和思政简单结合,而是需要根据具体课程的特点,精准地提取适宜的思政元素,并以恰当的方式将其融入教学过程。

2.1 思政元素的挖掘

目前,中心已经开设八个经典的物理化学实验项目。针对每个实验项目的独特性,详细整理相应的思政元素,具体内容如表1所示。

2.2 思政元素融入方式

探索多种思政元素融入方式,包括引导性问题设计、案例分析、探究式学习、项目实践等。这些方式可以有效地促进课程思政建设,让学生不仅能够掌握专业知识,还能够全面发展,增强社会责任感。例如,在“排水集气法测定过氧化氢催化分解反应的速率常数”实验中,过氧化氢在没有催化剂存在时,分解反应进行得很慢,但在碘化钾的催化作用下能够加快反应进程,但是不能改变反应产物。教师可以以提问的方式引导学生通过内因与外因的辩证关系解释此现象。内因是指反应本身的特性和性质,外因则是指外部引入的影响因素,如催化剂。在这个例子中,催化剂的引入改变了反应的外部条件,从而影响了反应的速率,但并不改变反应的最终产物。过氧化氢分解反应的进行受到内在的化学性质和能量要求的制约,未经催化剂作用时,反应速率较慢,这是由于分解过程中键的断裂需要消耗较大的能量,反应需要克服较高的活化能才能发生。碘化钾作为催化剂引入后,改变了反应的进程,提供了新的反应路径,使得反应的活化能降低。这样原本需要大量能量才能发生的反应,通过催化作用可以更容易地进行^[7]。

通过内因与外因的辩证关系解释这个例子,可以更清晰地理解催化剂在化学反应中的作用。在实验介绍时,教师可以为学生讲授我国老一辈科学家不求名利、潜心科研,为国家和社会的发展作出巨大贡献的事迹。例如,杰出科学家、教育家卢永根院士以不屈不挠的奋斗精神,将爱国奋斗的理念贯穿教学科研全过程,致力于水稻遗传育种研究,在半个多世纪的时间里,率领团队培育出33个作物新品种,推广种植面积1 000万亩以上,使之成为我国水稻种质资源的重要宝库之一,为国家农业发展和农业教育作出突出的贡献,表现出对党和国家的忠诚与对教育事业的深厚情怀。

表 1 物理化学实验内容中的思政元素

实验名称	思政元素简介
Fe(OH) ₃ 溶胶的制备与纯化实验	通过讨论铁离子在环境中的来源，引导学生思考资源合理利用和环境保护的重要性，培养学生的环保意识。引导学生思考实验过程中的安全问题，让他们了解实验操作的规范性和安全意识
界面电泳法测定溶胶的电动电势实验	探讨电泳技术在生物医学领域的应用，引导学生思考科学技术对社会发展的影响，培养他们的科研精神和创新意识。引导学生思考数据分析的重要性，培养他们的逻辑思维和判断能力
动态法测定液体的饱和蒸气压	引导学生思考液体蒸发与大气污染的关系，培养他们的环保意识和责任感。通过实验过程中对仪器操作的规范性要求，培养学生的安全意识和团队精神
电导法测定弱电解质的离解常数	探讨离解常数与溶解度的关系，引导学生思考溶解过程中离子的释放与水资源的合理利用。引导学生思考科学研究对解决社会问题的意义，培养学生的社会责任感和爱国情怀
旋光法测定蔗糖转化反应的速率常数	探讨光学活性物质在药物制备中的应用，引导学生思考科技创新对医疗事业的贡献，培养学生的创新意识和科研精神。引导学生思考研究数据的可靠性与结果的解释，培养学生的批判性思维能力和独立思考能力
排水集气法测定过氧化氢催化分解反应的速率常数	探讨催化剂在环境保护和能源利用中的重要作用，引导学生思考科技创新对社会可持续发展的推动作用，培养学生的创新意识和环保意识。引导学生思考数据处理的方法和结果的解释，培养学生的逻辑思维能力和批判性思维能力
对消法测定电池电动势	将实验内容与领悟习近平生态文明思想，理解和关心“双碳”战略、国家能源安全、环境保护、可持续发展和人民生命健康，体现“面向世界科技前沿、面向经济主战场、面向国家重大需求、面向人民生命健康”的要求紧密衔接，引导学生树立节约资源、保护环境的理念
最大泡压法测定溶液的表面张力	通过讲解表面张力在农业生产中的广泛应用，引出物理化学的实用性，增强学生的学习动力，例如：在农药和肥料喷洒方面，表面张力会影响液体在叶片表面的铺展程度；表面张力还被用于灌溉系统的设计等

总之，教师需要积极探索，挖掘物理化学实验课程中所蕴含的思想价值和精神内涵，结合实验教学内容寻找思政元素的融入点，注重启发性教育，以“润物细无声”的方式将思政教育潜移默化地融入物理化学实验教学。教师还应该积极组织并鼓励学生踊跃参加物理化学实验竞赛，依托竞赛提升学生的物理化学知识综合应用能力，提升学生的实践操作技能，并引导学生领会关于科技强国的重要精神，将个人理想追求升华到国家富强与民族复兴的层面，为实现中华民族伟大复兴的中国梦贡献力量。同时，中心建立“东区基础化学实验室”微信公众平台，发布前沿热点化学信息、实验室安全和我国杰出化学家事迹等内容，提升学生的思政素养^[8]。

3 结束语

在“双一流”建设背景下，课程思政建设在物理化学实验教学改革中十分必要。本文以思政团队建设、教学大纲完善、教学方法与手段选择、评价体系优化等四个方面进行物理化学实验课程思政建设的探，同时强调教师需要深入挖掘物理化学实验教学中蕴含的思政元素，不断优化完善思政元素在物理化学实验教学中的多角度融入，将专业教学与思政教育融为一体，让学生在掌握专业知识的同时接受思政教育，有效培养学生的爱国情怀、团队精神、科研精神、创新精神、环保意识、安全意识、

自主学习意识和综合全面发展意识等，成为对国家、对社会有用的创新型人才。

4 参考文献

[1] 孙晓环, 韩杰. “双一流”高校建设背景下物理化学基础实验教学改革研究 [J]. 广东化工, 2021, 48(17): 268, 275.

[2] 廖颖敏, 马嫻, 查晓松, 等. “双一流”背景下化学基础实验课程思政建设的探索 [J]. 广州化工, 2021, 49(24): 151-153.

[3] 孙越, 郝强, 周禹希. “双一流”背景下大学生科研创新能力的培养: 以物理化学实验教学为例 [J]. 辽宁师范大学学报(自然科学版), 2021, 44(1): 52-56.

[4] 张杰. 物理化学和物理化学实验课程思政元素的探索研究 [J]. 现代农村科技, 2022(8): 75-76.

[5] 李娟琴, 王静波, 任海生. 《物理化学》课程思政探索与实践 [J]. 广东化工, 2020, 47(24): 143-144.

[6] 王莉玮, 黄雅丽, 吴祥宗, 等. 产教融合背景下物理化学实验教学改革初探 [J]. 当代化工研究, 2022(8): 143-145.

[7] 尹常杰, 郑虹, 张秋禹, 等. 《物理化学实验》课程思政元素构建的探讨 [J]. 广州化工, 2023, 51(8): 263-264, 267.

[8] 卢晓南, 李青, 路千里, 等. 以学生为中心加强实验室文化建设 [J]. 实验室科学, 2016, 19(6): 202-204.

应用,新疆北部中职教育的培养目标和教学内容发生了较大变化。近年来,我国教育信息化已从1.0迈向2.0,中职教育在信息化层面也进入融合创新的阶段,未来的发展重点在于要实现信息化与中职教育的深度融合、实现虚拟平台与现实世界的动态融合、实现现代化意义上的校企融合等,以教育信息化的不断推进助力智慧校园建设,以智慧课堂、线上线下相结合的教学模式打破传统教学模式的桎梏,以虚拟现实技术推动互动远程教学模式的发展,重点解决难以直观化、受限于教学实验设备的问题,真正使中职教育适应数字经济时代的发展需求,切实将时代赋予中职教育的重任挑在肩上、落在实处^[4]。

3.3 提升新疆北部中职教育的人才竞争力

当今社会对中职教育所培养的人才要求越来越高。为了更好地适应市场需求,新疆北部中职教育需要提高人才培养质量,助力学生成为更具竞争力的人才。对于如何培养更多的高技能人才,国家明确指出,要进一步促进产教融合和校企合作,要以产业优化升级和技术改造为主要发展方向,促进教育链、产业链、创新链和人才链之间的有效衔接,从而吸引更多年轻人接受职业化的技能型、应用型教育。例如,在大数据和智能制造领域,新技术的应用可以帮助中职教育更好地引导学生掌握相关技能,从而增强毕业生的就业竞争力。应用新技术可

以为中职教育提供更好的平台和机会,促进学生创新能力和实践能力的培养^[5]。

4 结束语

在数字科技重塑全球经济与产业格局这一大背景下,智慧化发展无疑是中职教育发展的高端形态。当然,新技术在新疆北部中职教育领域的应用需要不断地探索和完善,既要积极思考发挥技术优势,又要规避技术弊端,从而推动新疆北部中职教育高质量发展。

5 参考文献

- [1] 曹晔,闫子靖.新时代现代职业教育的新格局、新目标[J].职业技术教育,2023,44(4):6-11.
- [2] 罗洁.新技术赋能未来教育[J].中小学信息技术教育,2021(6):26-29.
- [3] 刘邦奇,张金霞,许佳慧,等.智能技术赋能因材施教:技术框架、行业特点及趋势:基于智能教育行业发展实证数据的分析[J].电化教育研究,2021,42(2):70-77.
- [4] 汪燕,李慧玲.“面向2035”职业教育现代化的挑战、矛盾与战略图景构建[J].教育与职业,2019(16):18-24.
- [5] 曾欢,朱德全.新技术时代职业教育智慧课堂建设的逻辑框架[J].中国电化教育,2019(6):6-13.

— 欢迎订阅《中国教育技术装备》 —

· 中华人民共和国教育部主管 · 中国教育装备行业协会主办

《中国教育技术装备》(半月刊)每期定价16元,全年24期,年定价384元。上、下两期可分别在杂志社订阅,年定价均为192元。向本刊直接订阅,汇款后,请将填好的征订单发电子邮件到杂志社。统订需要分发的用户,发行部可代为分发邮寄,请将详细的分发地址、邮编、收件人姓名和电话,随征订单发电子邮件至杂志社。邮局订阅:请到邮局填写邮发代号82-975订阅(邮局只能全套订阅)。

联系人:甘 甜 联系电话:010-59893286 E-mail: cetea@163.com
杂志社官网: <http://www.cete1987.com>

银行汇款

户 名:《中国教育技术装备》杂志社
账 号:1100 1028 6000 5300 0206
开户行:中国建设银行北京白石桥支行



杂志社公众号



杂志订阅二维码



在线阅读小程序

检索证明

根据委托人提供的论文材料，委托人华南农业大学基础实验与实践训练中心 庄慧 1 篇论文收录情况如下表。

序号	论文名称	发表刊物及发表的年月卷期/页码等	作者排名	论文等级	作者文由单位	收录情况	影响因子	中科院大类分区
1	双一流建设背景下物理化学实验课程思政探索	中国教育技术装备 出版年：2024 卷期： 页码： - 文献号： 文献类型：	第一	普刊类	华南农业大学 基础实验与实践训练中心	CNKI	无	无

说明：论文等级和中科院大类分区按《华南农业大学学术论文评价方案（试行）》划分

报告免责声明：如未盖章，报告无效

华南农业大学图书馆



检素员：刘汉忠

2025-07-11

International Journal of Electrochemical Science

Volume 19, Number 8 (2024)





ScienceDirect®

International Journal of Electrochemical Science

Open access

3.6

CiteScore

2.4

Impact Factor

[Submit your article](#)

[Guide for authors](#)

Menu



Search in this journal

Volume 19, Issue 8

August 2024

[Download full issue](#)

[< Previous vol/issue](#)

[Next vol/issue >](#)

Receive an update when the latest issues in this journal are published

[Sign in to set up alerts](#)

[Contents list](#) [Open access](#)

Front Matter1:Full Title Page

Article 100724



[View PDF](#)

[Editorial board](#) [Open access](#)

Editorial Board

Article 100725



[View PDF](#)

[Review article](#) [Open access](#)

Modeling and simulation of a residential-based PEMFC-CHP system

Xin Zhang, Lingyi Xu, Long Zou, Ziheng Jiang, ... Qiuwan Shen

Article 100638



[View PDF](#)

[Article preview](#)

[FEEDBACK](#)

Research article *Open access*

Preparation of lithium ferromanganese phosphate by non-stoichiometric strategy

Hui Zhuang, Jie Wang

Article 100636



[View PDF](#)

Article preview

Research article *Open access*

Evaluation of hydration behavior of cement-stabilized macadam via electrochemical impedance spectroscopy

Duo Wu, Yuxue Yin, Tao Fu, Hongyan Sun, Fuming Liu

Article 100640



[View PDF](#)

Article preview

Research article *Open access*

High-sensitivity ammonia gas sensor based on hollow microsphere MXene@SnS₂@polyaniline composite material with humidity resistance

Xiaojuan Zhao, Lin Lu, Yongjin Zou, Fen Xu, ... Cuili Xiang

Article 100658



[View PDF](#)

Article preview

Research article *Open access*

Co nanoparticle-loaded porous carbon for high-performance supercapacitors

Dongmei Zhao, Jiayuan Hu, Jiying Shi, Yanmei Zhao, Zhanpeng Xu

Article 100652



[View PDF](#)

Article preview

Research article *Open access*

Dendrite-free and highly stable Zn metal anode with ZIF-8 ions-transport layer

Jianming Han, Xiaozhou Ye, Hui Yang, Jiazhou Tao, ... Yiting Peng

Article 100655



[View PDF](#)

Article preview

Research article *Open access*

Design a polymer-based composite electrolyte with high ionic conductivity for high-performance lithium-metal batteries

Nankun Geng, Tongtong Xu, Xinhao Xu, Shasha Zhu, ... Qunjie Xu

Article 100656



[View PDF](#)

Article preview

Research article *Open access*

Effect of MoS₂ nanoparticles on the properties of Ni-W-SiC composite coatings

Huizhong Ma, Yu Feng, Na Li, Cong Tan, Lan Zhang

Article 100654

 [View PDF](#) [Article preview](#) ✓

Research article *Open access*

Influence of welding defects on hydrogen embrittlement sensitivity of girth welds in X80 pipelines

Bei Wang, Quan Liu, Qingshan Feng, Xiuyun Wang, ... Jianxing Chen

Article 100661

 [View PDF](#) [Article preview](#) ✓

Research article *Open access*

Research on SOC estimation of lithium-ion batteries based on robust full order proportional integral observer

Yongchao Wang, Chunyan Li, Qin Sun, Yujia Chang

Article 100645

 [View PDF](#) [Article preview](#) ✓

Research article *Open access*

Optimization of the electrolytic polishing parameters of intravascular stent based on the orthogonal test method

Yongqi Wang, Xuemin Jing, Yang Li, Xuefeng Zhang, ... Xiuting Wei

Article 100648

 [View PDF](#) [Article preview](#) ✓

Research article *Open access*

Evolutionary trends and research hotspots in electrochemical machining: A bibliometric analysis from 2010 to 2023

Feng Ji, Yuan An, Yawen Xin, Haoran Guan

Article 100646

 [View PDF](#) [Article preview](#) ✓

Research article *Open access*

Experimental and theoretical studies on the electrochemical behavior of Al alloy treated by cyclohexanol-based inhibitor

Adam Nid-bella, Bouchra Es-Sounni, Mohamed Bakhouch, Aisha H. Al-Moubaraki, ... Young Gun Ko

Article 100651

 [View PDF](#) [Article preview](#) ✓

Research article *Open access*

Influence of electric field, liquid film thickness, and sodium chloride deposition on atmospheric corrosion of Cu

Rongdie Zhu, Jinyang Zhu, Hongbin Zhang, Binxia Ma, Shaofeng Zhang

Article 100650

 [View PDF](#) [Article preview](#) ✓

Research article *Open access*

Computational study of the carbon steel corrosion behaviors under alternating current based on the mathematical model

Shouxin Zhang, Yuanyu Wang, Chunhao Ye

Article 100660



[View PDF](#)

[Article preview](#)

Research article *Open access*

Acquisition and recognition of *Lycoris spp.* fingerprint patterns using artificial intelligence-enhanced electrochemical sensors

Xiantu Lin

Article 100674



[View PDF](#)

[Article preview](#)

Research article *Open access*

Molecularly imprinted sensors for the determination of anthocyanins in food products

Juanjuan Wang, Yong Qin

Article 100673



[View PDF](#)

[Article preview](#)

Research article *Open access*

Research and development of double layer P-doped laser induced graphene thin film electrode for flexible micro-supercapacitor applications

Xing Liu, Ruiwei Wang, Cong Wang, Hongyu He, ... Junli Yin

Article 100653



[View PDF](#)

[Article preview](#)

Research article *Open access*

Facile fabrication of mesoporous Ag-doped γ -MnO₂ nanowires with rich oxygen defects for boosting performance of aqueous Zn-ion batteries

Ying Li, Junjie You, Zhuotong Yu, Chuanqing Du, ... Siqing Cheng

Article 100663



[View PDF](#)

[Article preview](#)

Research article *Open access*

Influence of trapezoidal channel design on volume power density of ammonia-hydrogen fuel cells

Jinyi Hu, Yongbao Liu, Xing He, Jianfeng Zhao

Article 100676



[View PDF](#)

[Article preview](#)

Research article *Open access*

Numerical modelling of an effective perovskite solar cell and PV-module for comparison analysis of organic and inorganic electron transport layers

Adnan Javed, Muhammad Farooq Nasir, Irfan Qasim, Yousef Mohammed Alanazi, Muhammad Tahir Khan
Article 100641



[View PDF](#)

Article preview

Review article *Open access*

Electrochemical sensors and biosensors: effective tools for detecting heavy metals in water and food with possible implications for children's health

Liliana Anchidin-Norocel, Gheorghe Gutt, Elena Tătăranu, Sonia Amariei

Article 100643



[View PDF](#)

Article preview

Research article *Open access*

Synthesis, structural characterisations, electrochemical behavior and antibacterial activities of a chromium(III) resorcinolate complex

Tigist Tsega, Getasil Chanie, Adane Kassa, Mamo Gebrezgiabher, ... Atakilt Abebe

Article 100659



[View PDF](#)

Article preview

Research article *Open access*

Defect transport and thermal mismatch induced fracture in planar solid oxide fuel cell

Sen Yang, Yongjun Lu, Kejie Wang, Xiang Zhao, Fenghui Wang

Article 100678



[View PDF](#)

Article preview

Research article *Open access*

Electrodeposition of Pb-0.6%Sb/ α -PbO₂/ β -PbO₂-CNTs electrodes: Investigation focusing on co-deposition modification mechanism and energy consumption

Bohao Yu, Ruidong Xu, Xuanbing Wang, Buming Chen, Yunbo Yang

Article 100679



[View PDF](#)

Article preview

Research article *Open access*

The impact of glycerol polyoxyethylene ether on the characteristics of lithium iron phosphate pastes and their electrochemical performance

Kang Liu, Xin Chen, Jinglong Chen

Article 100604



[View PDF](#)

Article preview

Research article *Open access*

Enhanced corrosion protection of copper alloy in 2.0M HNO₃ solution using expired solo sept, slim-lax and well derm drugs

R.N. Felaly, M. Alfakeer, Asmaa A.I. Ali, Salih S. Al-Juaid, ... M. Abdallah

Article 100657

 [View PDF](#) [Article preview](#) ✓

Research article *Open access*

Exploring *Ginkgo biloba* extract's green corrosion inhibition effects on Q235 steel in H₂SO₄ environments

Xuewei An, Jingjing Dai, Shu Wang, Wenda Zou

Article 100677

 [View PDF](#) [Article preview](#) ✓

Research article *Open access*

State of health estimation method based on real data of electric vehicles using federated learning

Xiaoxin Lv, Yi Cheng, Shidian Ma, Haobin Jiang

Article 100591

 [View PDF](#) [Article preview](#) ✓

Research article *Open access*

Polyaniline/titanium phosphate as a biosensor detection of glucose performance

Israa Khalil Sultan, Zaid H. Mahmoud

Article 100671

 [View PDF](#) [Article preview](#) ✓

Research article *Open access*

Study on the ablation process and failure mechanism of the buffer layer in high-voltage XLPE cable

Yi Tian, Guixin Zhu, Qingqing Miao, Jiasheng Huang, ... Licheng Li

Article 100662

 [View PDF](#) [Article preview](#) ✓

Research article *Open access*

Enhancing microscale additive manufacturing: Electrolyte-column localized electrochemical deposition for microwire and microdevice substrate connection

Ge Qin, Lei Han, Shiwei Li, Shen Niu, ... Pingmei Ming

Article 100683

 [View PDF](#) [Article preview](#) ✓

Short communication *Open access*

Facile synthesis of LiFePO₄/Cu composite as enhanced cathode material for lithium-ion battery by a solid-state grinding method

Rusi Hao, Wenliang Sun

Article 100684

 [View PDF](#) [Article preview](#) ✓

Research article *Open access*

Electrochemical high sensitive detection of hydrogen peroxide based on platinum-palladium nano-enzyme modified microelectrode

Sitian Zhao, Long Chen, Wenjie Luo, Zijie Pi, ... Xiaoling Liao

Article 100672



[View PDF](#)

Article preview

Short communication *Open access*

Study on the influence of pulse electrodeposition parameters on corrosion resistance of CoCr alloy in simulated concrete pore solution

Zhang Wenbin, Wei Lidan

Article 100682



[View PDF](#)

Article preview

Research article *Open access*

An electrochemical analysis of green corrosion inhibitor for A335 pipe steel in produced water media

Anaum Nawaz, Kashif Mairaj Deen, Shabib Ishraq, Waseem Haider

Article 100680



[View PDF](#)

Article preview

Research article *Open access*

Preparation of hierarchical porous carbon materials from bamboo shoot shells via air activation for high-performance supercapacitors

Fanen Zeng, Yaning Zhang, Qi Lv, Lu Lu, Bing Xu

Article 100691



[View PDF](#)

Article preview

Research article *Open access*

Detection and intelligent optimization of blood glucose signals based on MXene-assisted sensors

Minrui Bai, Yuxiao Zhou, Shilei Deng

Article 100687



[View PDF](#)

Article preview

Research article *Open access*

Corrosion characteristic of vitallium 2000 CoCrMo casting alloy in fluoride containing artificial saliva

Mingmin Zhu, Jing Wang, Yanxiao Zhang, Jie Wang, ... Ming Liu

Article 100690



[View PDF](#)

Article preview

Short communication *Open access*

Direct electrocatalytic sensing of myoglobin using an annealed Au-implanted electrode

Fenfen Liang, Yanhong Zhang, Mingxia Zhao, Junbing Jiang

Article 100681



[View PDF](#)

Article preview

Research article *Open access*

High-performance electrocatalysts based core-shell SWCNHs@ZIF-67 heterostructure for ultrasensitive H₂O₂ sensing

Yile Hu, Jingge Shi, Zifan Wang, Xiaopeng Wang, ... Hui Yang

Article 100689



[View PDF](#)

[Article preview](#)

Research article *Open access*

Cobalt-based selenide composite materials as high-efficiency electrocatalysts for oxygen evolution reaction

Feng Ao, Tengfei Meng, Yujun Zhu, Kai Huang, Yupei Zhao

Article 100696



[View PDF](#)

[Article preview](#)

Research article *Open access*

Eco-friendly corrosion inhibition of steel in acid pickling using Prunus domestica Seeds and Okra stems extracts

B.A. Abd-El-Nabey, M.E. Mohamed, A.M. Helmy, H. Elnagar, A.M. Abdel-Gaber

Article 100695



[View PDF](#)

[Article preview](#)

Research article *Open access*

Incorporating different enzyme kinetics in amperometric biosensor for the steady-state conditions: A complete theoretical and numerical approach

Jeyaramar Arul Vinayagan, Subburaj Murali Krishnan, Lakshmanan Rajendran, Alagu Eswari

Article 100693



[View PDF](#)

[Article preview](#)

Research article *Open access*

Hydrothermal synthesis of α₁LiVOPO₄ as a cathode material for Li-ion batteries

Jingjing Cai, Guanhua Jin, Fang Zhang, Yanfei Zeng, Hongyu Li

Article 100637



[View PDF](#)

[Article preview](#)

Research article *Open access*

Electrochemical deposition and characterization of cuprous oxide crystallites on stainless substrates: Growth mechanism and morphological analysis

Yi Hu, Pin Syuan Chen, Yi-Chun Ko, Cheng Han Tsai

Article 100688



[View PDF](#)

[Article preview](#)

Research article *Open access*

Corrosion behavior of Mg–Bi–Ca alloys prepared via high vacuum melting as biodegradable materials in Hank solution

A. Torres-Islas, A. Bedolla-Jacuinde, A. Del-Pozo, C. González- Loyola, ... H. Martinez

Article 100692



[View PDF](#)

Article preview

Review article *Open access*

Triboelectric nanogenerator for ocean energy harvesting: A review of technological advances and future perspectives

Bingqiang Shan, Tengtian Ai, Kai Wang

Article 100694



[View PDF](#)

Article preview

Research article *Open access*

Investigating the magnetohydrodynamics non-Newtonian fluid movement on a tensile plate affected by variable thickness with dufour and soret effects: Akbari Ganji and finite element methods

Milad Sadinezhad Fard, Abolfazl Torabiyani, Payam Jalili, Bahram Jalili, Davood Domiri Ganji

Article 100701



[View PDF](#)

Article preview

Research article *Open access*

Corrosion resistance of zinc-magnesium-aluminium alloy coated steel in marine atmospheric environments

Degao Qiao, Shuliu Wang, Peidong Ning, Qianqian Liu, ... Kui Xiao

Article 100705



[View PDF](#)

Article preview

Research article *Open access*

Investigation of quality control of Gastrodia elata using electrochemical fingerprint technology

Yufei Liao, Ping Wang, Ruirui Zhang, Geyu Chen, Jiale Fu

Article 100702



[View PDF](#)

Article preview

Research article *Open access*

Ag-Au bimetallic nanoparticle-based electrochemical sensing platform for quantification of B-type natriuretic peptide

Yuanli Zhang, Meilan Sun

Article 100703



[View PDF](#)

Article preview

Research article *Open access*

Electrochemical detection strategies for cardiovascular disease biomarkers: Applications in troponin I and troponin T assays

Zhijun Li, Aiqin Zhong

Article 100675



[View PDF](#)

Article preview

Research article *Open access*

Synthesis and properties optimization of $\text{Na}_3(\text{VOPO}_4)_2\text{F}$ cathode material for sodium-ion batteries by co-precipitation method

Xiaoping Yang, Wenjiao Li, Jianguo Duan, Yanan Xin, ... Ding Wang

Article 100704



[View PDF](#)

[Article preview](#)

Research article *Open access*

Evaluation of corrosion resistance and self-healing performance of phytic acid-vanadate composite coating on Q235 steel

Yong Lu, Huixia Feng, Xia Hou

Article 100700



[View PDF](#)

[Article preview](#)

Research article *Open access*

Preparation of MoSi_2 -particle reinforced Ni-W alloy coatings and their anti-corrosion behavior in CO_2 -saturated 3.5% NaCl solution

Hongjie Li, Shaomu Wen, Zhiming Yu, Junkun Hu, ... Xudong Ren

Article 100708



[View PDF](#)

[Article preview](#)

Research article *Open access*

The inhibitive action of lemon verbena plant extract as an economical and eco-friendly corrosion inhibitor for mild steel in acidic solutions

Ghazal Sadat Sajadi, Fatemeh Salmanian, Raziieh Naghizade, Seyed Mohammad Ali Hosseini

Article 100699



[View PDF](#)

[Article preview](#)

Research article *Open access*

Efficient electrochemical synthesis of phenylacetic acid derivatives: Utilizing CO_2 for sustainable production

Wenhui Dong, Xinyuan Sun, Qianqian Niu, Yun Zhu, Baokang Jin

Article 100709



[View PDF](#)

[Article preview](#)

Research article *Open access*

Titanium surface treatments and their effects on the roughness factor

Leonardo Salgado, Teresa Zayas, Clara B. Rodríguez, Guillermo Soriano-Moro, Víctor H. Lara

Article 100697



[View PDF](#)

[Article preview](#)

Research article *Open access*

Excellent inhibition performance of an imidazole based ionic liquid on steel-N80 in 15% hydrochloric acid medium

Chaoqun Wang, Huasha Liu, Yu Wan, Yusheng Li, ... Lei Guo

Article 100712



[View PDF](#)

[Article preview](#)

Research article *Open access*

Initial corrosion behavior of 10CrNi3MoV steel and Q235 steel in marine atmosphere

Zhixian Gao, Jingwang Niu, Guoqing Ding, Jifeng Ding, ... Xiangyang Li

Article 100707



[View PDF](#)

[Article preview](#)

[< Previous vol/issue](#)

[Next vol/issue >](#)

About this publication

ISSN: 1452-3981

Copyright © 2025 ESG. Published by Elsevier B.V. All rights are reserved, including those for text and data mining, AI training, and similar technologies.



ELSEVIER

All content on this site: Copyright © 2025 Elsevier B.V., its licensors, and contributors. All rights are reserved, including those for text and data mining, AI training, and similar technologies. For all open access content, the relevant licensing terms apply.





Preparation of lithium ferromanganese phosphate by non-stoichiometric strategy

Hui Zhuang^{a,*}, Jie Wang^b

^a Experimental Basis and Practical Training Center, South China Agricultural University, Guangzhou 510642, China

^b School of Chemistry and Chemical Engineering, South China University of Technology, Guangzhou 510640, China

ARTICLE INFO

Keywords:

LIBs
Non-stoichiometric
Cathode
 $\text{Li}_x\text{Fe}_x\text{Mn}_{1-x}\text{PO}_4$
Solid-phase method

ABSTRACT

$\text{Li}_x\text{Fe}_x\text{Mn}_{1-x}\text{PO}_4$ exhibits low production costs, environmental friendliness, high energy density, thermal stability, and cycling stability in lithium-ion batteries (LIBs), presenting broad application prospects. Furthermore, studies have shown that adopting a non-stoichiometric ratio strategy can reduce particle size, decrease anti-site defects, and generate a conductive impurity phase on the material surface. This leads to an enhancement in the electrochemical performance of the material, making it an effective approach to achieving high-performance olivine-type cathode materials. In this study, three materials were successfully prepared using the solid-phase method: $\text{Li}_{1.05}\text{Fe}_{0.5}\text{Mn}_{0.475}\text{PO}_4/\text{C}$, $\text{Li}_{1.05}\text{Fe}_{0.5}\text{Mn}_{0.5}\text{PO}_4/\text{C}$, and $\text{Li}_{1.05}\text{Fe}_{0.475}\text{Mn}_{0.5}\text{PO}_4/\text{C}$. The physical properties of the materials were characterized using X-ray diffraction (XRD), transmission electron microscopy (TEM), and scanning electron microscopy (SEM). The electrochemical performance including specific capacity, rate performance, and cycling performance were studied through charge-discharge tests, with $\text{Li}_{1.05}\text{Fe}_{0.5}\text{Mn}_{0.475}\text{PO}_4/\text{C}$ exhibiting the best specific capacity at all rates. At rates of 0.1 C, 0.5 C, 1 C, 2 C, and 5 C, its average reversible specific capacities were 143.5, 129.5, 122.1, 112.8, and 97.3 $\text{mAh}\cdot\text{g}^{-1}$, respectively. Furthermore, differences in electrochemical performance of three materials were discussed in detail through cyclic voltammetry (CV) and electrochemical impedance spectroscopy (EIS).

1. Introduction

LiMPO_4 ($\text{M} = \text{Fe}, \text{Mn}, \text{Mn}_y\text{Fe}_{1-y}, \text{Co}, \text{Ni}, \text{V}$) materials have become the most commercially valuable cathode materials for lithium-ion batteries due to their characteristics of non-toxicity, pollution-free, good safety, wide availability of raw materials, low cost, and long lifespan [1]. The $\text{LiFe}_x\text{Mn}_{1-x}\text{PO}_4$ ($0 < x < 1$) solid solution material utilizes the synergistic effect of iron and manganese elements, combining the higher conductivity of LiFePO_4 with the higher voltage platform of LiMnPO_4 [2], thus exhibiting high competitiveness in LIBs cathode materials. The high-temperature solid-phase method, with its simple process, low cost, and high yield, has become one of the most commonly used methods for industrial-scale production of $\text{LiFe}_x\text{Mn}_{1-x}\text{PO}_4$ materials.

However, olivine-structured phosphate compounds themselves have some inherent drawbacks, such as lower electron conductivity and one-dimensional slow lithium-ion diffusion rate, which limit the electrochemical performance of $\text{LiFe}_x\text{Mn}_{1-x}\text{PO}_4$ materials and further applications. Researchers have designed many effective modification strategies through extensive experimental studies, including

nanoparticle size reduction, coating with conductive materials, ion doping, and material structure design and morphology control [3]. Meanwhile, through the study of LiFePO_4 , it has been found that the design of non-stoichiometric ratios can effectively enhance the electrochemical performance of the materials [4]. However, current research on non-stoichiometric $\text{LiFe}_x\text{Mn}_{1-x}\text{PO}_4$ materials remains relatively limited. Based on our research on $\text{LiFe}_{0.5}\text{Mn}_{0.5}\text{PO}_4$ materials [5], we aim to investigate the influence of non-stoichiometry on the electrochemical properties of $\text{Li}_x\text{Fe}_x\text{Mn}_{1-x}\text{PO}_4$ materials. We adopted a solid-phase method conducive to industrial production to prepare a series of non-stoichiometric $\text{Li}_x\text{Fe}_x\text{Mn}_{1-x}\text{PO}_4$ samples with carbon coating building upon previous methodologies. Subsequently, we analyzed the influence of non-stoichiometric design on the material's phase composition, morphological structure, and electrochemical performance.

* Corresponding author.

E-mail address: zhzh@scau.edu.cn (H. Zhuang).

<https://doi.org/10.1016/j.ijoes.2024.100636>

Received 20 March 2024; Received in revised form 6 May 2024; Accepted 6 May 2024

Available online 17 May 2024

1452-3981/© 2024 The Author(s). Published by Elsevier B.V. on behalf of ESG. This is an open access article under the CC BY-NC-ND license (<http://creativecommons.org/licenses/by-nc-nd/4.0/>).

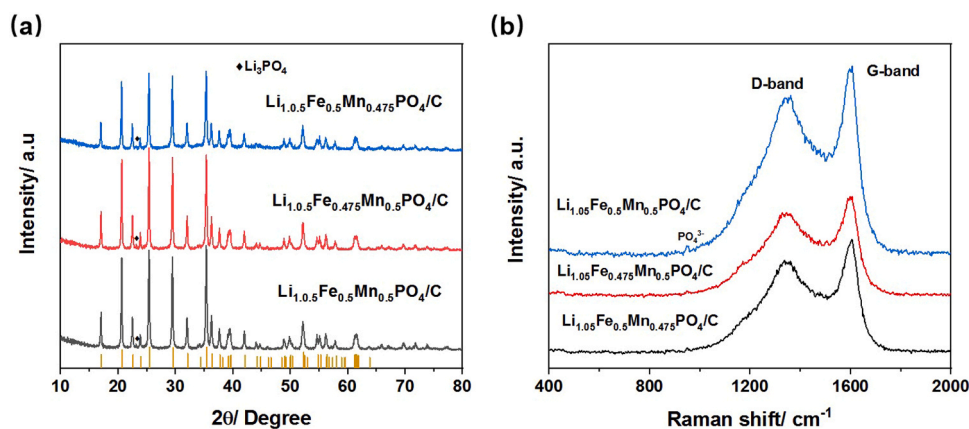


Fig. 1. (a) XRD patterns and (b) Raman spectra of $\text{Li}_{1.05}\text{Fe}_{0.5}\text{Mn}_{0.5}\text{PO}_4/\text{C}$, $\text{Li}_{1.05}\text{Fe}_{0.475}\text{Mn}_{0.5}\text{PO}_4/\text{C}$ and $\text{Li}_{1.05}\text{Fe}_{0.5}\text{Mn}_{0.475}\text{PO}_4/\text{C}$ samples.

2. Experimental section

2.1. Chemical reactants

LiH_2PO_4 (AR), MnCO_3 (AR), $\text{FeC}_2\text{O}_4 \cdot 2\text{H}_2\text{O}$ (AR), Li_2CO_3 (AR), polyvinyl alcohol (AR), oleic acid (AR), sucrose (AR) were purchased from Aladdin Reagent (Shanghai) Co., Ltd. The above reagents were used directly without purification.

2.2. Preparation of $\text{Li}_x\text{Fe}_x\text{Mn}_{1-x}\text{PO}_4$ samples

The $\text{Li}_x\text{Fe}_x\text{Mn}_{1-x}\text{PO}_4$ samples were synthesized by a ball-milling solid-state route assisted with surfactant agent (oleic acid). In a general experiment: 1.5 mL of oleic acid was dissolved into 30 mL of ethanol firstly. Then LiH_2PO_4 , $\text{FeC}_2\text{O}_4 \cdot 2\text{H}_2\text{O}$, MnCO_3 , and Li_2CO_3 were weighed in a molar ratio of 0.2:0.1:0.1:0.01, respectively. And an equal quantity of sucrose and polyvinyl alcohol (used as carbon sources) were added into the ethanol solution. After ball milling for 8 h under the rate of 400 rpm, the final mixture in ultrafine powder obtained from decantation/filtration was dried by vacuum at 60 °C and transferred into a tube furnace. Finally, the ultrafine powder was heated to 420 °C with a heating rate of 5 °C·min⁻¹ and maintained for another 1 h at this temperature in an Ar atmosphere. After that, the calcination temperature was increased to 650 °C using the same heating rate and remained for 8 h to achieve the $\text{Li}_{1.05}\text{Fe}_{0.5}\text{Mn}_{0.5}\text{PO}_4/\text{C}$ sample. Specifically, altering the molar ratio to 0.2:0.095:0.1:0.01 and 0.2:0.1:0.095:0.01 achieved the $\text{Li}_{1.05}\text{Fe}_{0.475}\text{Mn}_{0.5}\text{PO}_4/\text{C}$ and $\text{Li}_{1.05}\text{Fe}_{0.5}\text{Mn}_{0.475}\text{PO}_4/\text{C}$ samples, respectively.

2.3. Characterizations

XRD patterns of the as-prepared samples were tested on a Bruker D8 ADVANCE diffractometer, using a Cu K α radiation source ($\lambda = 1.5406 \text{ \AA}$). The Raman spectrum was performed on a Bio-Rad FTS6000 Raman spectroscopy with a 532 nm blue laser beam. Particle sizes, morphologies, and crystal structures of the as-prepared samples were observed by Zeiss field-emission SEM. The thickness of the carbon layer on the surface was determined using a JEOL-2100 TEM. N_2 adsorption/desorption isotherms were determined by Brunauer–Emmett–Teller (BET) measurement using a BeiShiDe 3 H-2000PS1 surface area analyzer at the temperature of 77 K. The pore size distribution (PSD) was calculated from the adsorption branch of the pore size distribution curve obtained via the Barrett–Joyner–Halenda (BJH) method.

2.4. Electrochemical measurements

To evaluate the electrochemical performance of the $\text{Li}_x\text{Fe}_x\text{Mn}_{1-x}\text{PO}_4$ samples, electrodes were prepared by mixing 80 wt% $\text{Li}_x\text{Fe}_x\text{Mn}_{1-x}\text{PO}_4$,

10 wt % acetylene black, and 10 wt % polyvinylidene fluoride (PVDF) on an aluminum foil using a tape-casting technique. Coin cells (CR2025) were assembled with the $\text{Li}_x\text{Fe}_x\text{Mn}_{1-x}\text{PO}_4$ electrode as the cathode and lithium metal foil as the anode. The electrolyte used was a 1.0 M LiPF_6 solution in ethylene carbonate/ethylene methyl carbonate (EC-EMC = 1:1 v/v), and Celgard 2500 was employed as the separator within an Ar-filled glove box. Each electrode was loaded with approximately 2.5 mg·cm⁻² of the $\text{Li}_x\text{Fe}_x\text{Mn}_{1-x}\text{PO}_4$ composite. The cells underwent cycling between 2.0 and 4.5 V vs. Li/Li^+ at various current densities using a multichannel battery test system (NEWARE CT-3008 W) with a constant-current (CC-) protocol. Specific capacity calculations were conducted based on the total mass of the $\text{Li}_x\text{Fe}_x\text{Mn}_{1-x}\text{PO}_4$ composite.

CV measurements were performed using an electrochemical workstation (CHI 760D) at various sweep rates ranging from 2.0 to 4.5 V vs. Li/Li^+ . EIS data were acquired from coin cells subjected to a specific number of cycles using a CHI 760D electrochemical workstation at room temperature, with a 10 mV excitation potential and frequencies ranging from 100 kHz to 10 mHz. Impedance spectra were analyzed using an equivalent circuit (as depicted in the inset figure). These spectra exhibited a minor intercept in the high-frequency range, a semicircle at high-to-medium frequencies, and a sloping line in the low-frequency range. The high-frequency intercept represented the uncompensated resistance (R_s), which includes electrolyte resistance, particle-particle contact resistance, and resistance between the electrode and current collector [6]. The semicircle at high-to-medium frequencies was ascribed to charge transfer resistances (R_{ct}) at the electrode/electrolyte interface [7]. Meanwhile, the inclined line in the low-frequency region corresponded to the Warburg impedance (W_o), which indicates lithium ion diffusion within the electrodes [8].

3. Results and discussion

Fig. 1a illustrates the XRD patterns of the three samples, all of which exhibit diffraction peaks aligned with the standard card PDF#42–0580, corresponding to the orthorhombic Pnmb space group. Impurity peaks attributed to Li_3PO_4 are detected within the 2θ range of 22° to 24° for all samples, with the lowest intensity observed in $\text{Li}_{1.05}\text{Fe}_{0.5}\text{Mn}_{0.475}\text{PO}_4/\text{C}$, indicating relatively lower impurity content in this sample. The Raman spectra, depicted in Fig. 1b, reveals a faint absorption peak at 948 cm⁻¹, attributed to the characteristic absorption of PO_4^{3-} , suggesting a sufficiently thin surface carbon layer to permit light penetration. Notably, two prominent absorption peaks at 1340 and 1600 cm⁻¹ correspond to the D and G bands of amorphous carbon, respectively. The ratio of the intensities of these bands (I_D/I_G) serves as an indicator of the degree of graphitization of the carbon layer, with lower I_D/I_G ratios indicative of enhanced graphitization and improved material conductivity [9]. Specifically, the I_D/I_G values for the $\text{Li}_{1.05}\text{Fe}_{0.5}\text{Mn}_{0.5}\text{PO}_4/\text{C}$, $\text{Li}_{1.05}\text{Fe}_{0.475}\text{Mn}_{0.5}\text{PO}_4/\text{C}$, and $\text{Li}_{1.05}\text{Fe}_{0.5}\text{Mn}_{0.475}\text{PO}_4/\text{C}$ materials are 0.867, 0.858,

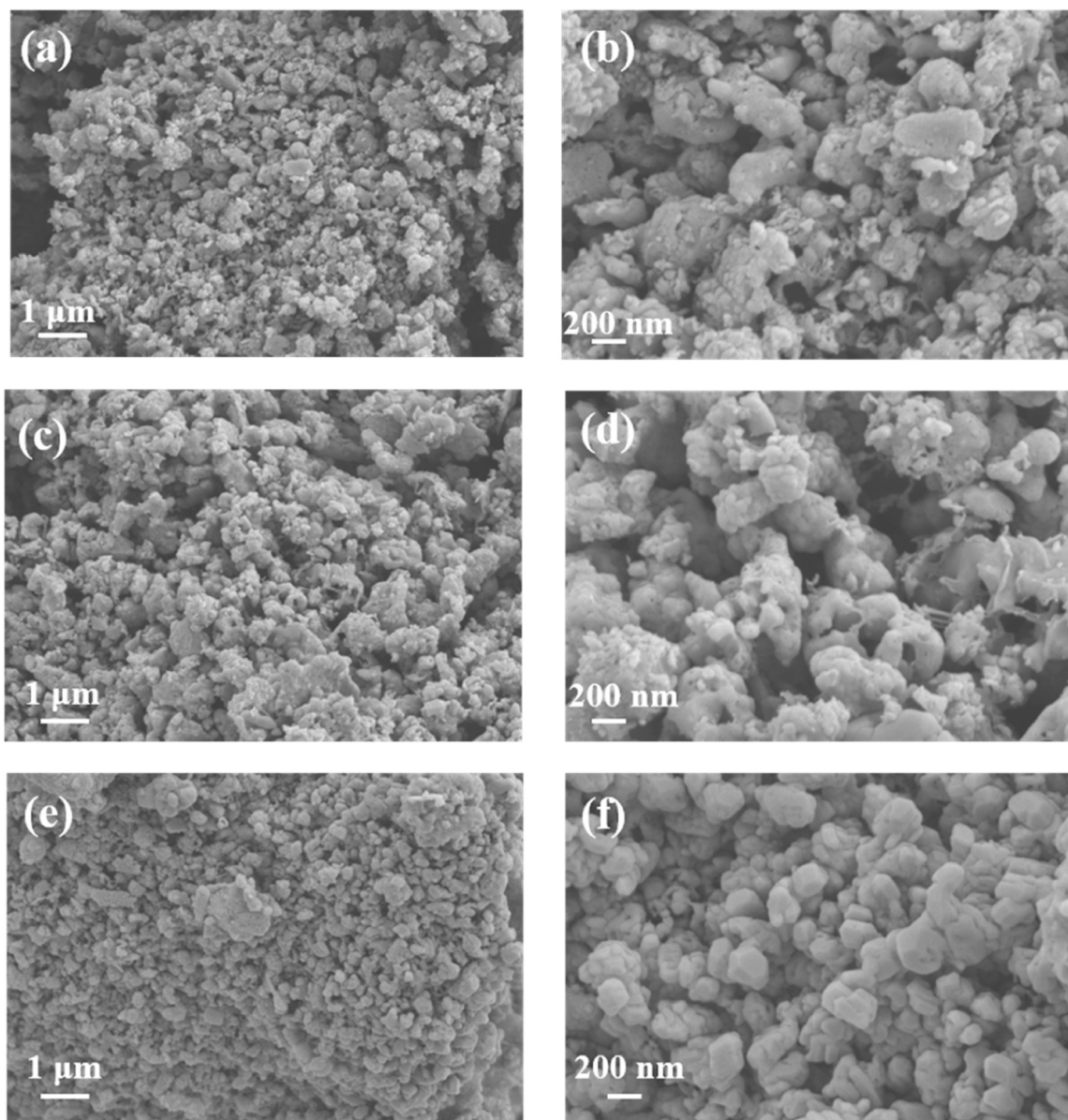


Fig. 2. SEM images of (a,b) $\text{Li}_{1.05}\text{Fe}_{0.5}\text{Mn}_{0.5}\text{PO}_4/\text{C}$, (c,d) $\text{Li}_{1.05}\text{Fe}_{0.475}\text{Mn}_{0.5}\text{PO}_4/\text{C}$ and (e,f) $\text{Li}_{1.05}\text{Fe}_{0.5}\text{Mn}_{0.475}\text{PO}_4/\text{C}$.

and 0.831, respectively, suggesting that the $\text{Li}_{1.05}\text{Fe}_{0.5}\text{Mn}_{0.475}\text{PO}_4/\text{C}$ material exhibits the highest conductivity among the three samples.

Fig. 2 illustrates the SEM images of three samples. All three samples consist of primary particles aggregating to form secondary particles with a broad size distribution. In $\text{Li}_{1.05}\text{Fe}_{0.5}\text{Mn}_{0.5}\text{PO}_4/\text{C}$ and $\text{Li}_{1.05}\text{Fe}_{0.475}\text{Mn}_{0.5}\text{PO}_4/\text{C}$ samples, there are numerous small particles resulting in a noticeable increase in particle size for both samples. In contrast, the surface of $\text{Li}_{1.05}\text{Fe}_{0.475}\text{Mn}_{0.5}\text{PO}_4/\text{C}$ appears smoother but exhibits more severe cross-linking, resulting in an increase in average particle size. The morphology of $\text{Li}_{1.05}\text{Fe}_{0.5}\text{Mn}_{0.475}\text{PO}_4/\text{C}$ is markedly different, with smooth surface exhibiting polyhedral shapes, smaller size, and a more uniform distribution. The mechanism behind the morphological changes of $\text{Li}_{1.05}\text{Fe}_{0.5}\text{Mn}_{0.475}\text{PO}_4/\text{C}$ remains unclear. However, maintaining the total valence of cations unchanged, and appropriately reducing the Mn content might be a strategy for modulating the morphology of material. TEM images (Fig. 3) reveal that the surfaces of $\text{Li}_{1.05}\text{Fe}_{0.5}\text{Mn}_{0.475}\text{PO}_4/\text{C}$ are covered with a carbon coating layer of ~ 2 nm thickness. This carbon layer prevents direct contact between the electrolyte and the active material, thereby enhancing the conductivity of the material.

The ICP-OES testing was conducted on $\text{Li}_{1.05}\text{Fe}_{0.5}\text{Mn}_{0.475}\text{PO}_4/\text{C}$ to

ascertain the actual content of each constituent element. The results (Table 1) indicate that the Li, Fe, and Mn content aligns closely with theoretical expectations.

Fig. 4 illustrates the nitrogen adsorption-desorption curves and pore size distribution of the three materials, three samples all exhibit hysteresis loops of type H3, which are indicative of Type IV adsorption isotherms. The BJH pore size distribution tests reveal similar pore size distributions for three samples, primarily ranging from 3 to 50 nm. BET analysis indicates that the specific surface areas of $\text{Li}_{1.05}\text{Fe}_{0.5}\text{Mn}_{0.5}\text{PO}_4/\text{C}$, $\text{Li}_{1.05}\text{Fe}_{0.475}\text{Mn}_{0.5}\text{PO}_4/\text{C}$ and $\text{Li}_{1.05}\text{Fe}_{0.5}\text{Mn}_{0.475}\text{PO}_4/\text{C}$ are 30.03, 27.69, and $30.45 \text{ m}^2\cdot\text{g}^{-1}$, respectively. The specific surface area of $\text{LiFe}_x\text{Mn}_{1-x}\text{PO}_4$ materials is directly correlated with carbon content and particle size, significantly influencing the electrochemical performance of the materials. Elemental analysis confirms that all three materials have similar carbon contents. SEM observations, however, reveal that the particle size of $\text{Li}_{1.05}\text{Fe}_{0.5}\text{Mn}_{0.475}\text{PO}_4/\text{C}$ is noticeably smaller with a more regular morphology. Results calculated using Jade software also demonstrate that $\text{Li}_{1.05}\text{Fe}_{0.5}\text{Mn}_{0.475}\text{PO}_4/\text{C}$ has the smallest average particle size, which explains the slight increase in specific surface area observed in this sample. The increased specific surface area provides

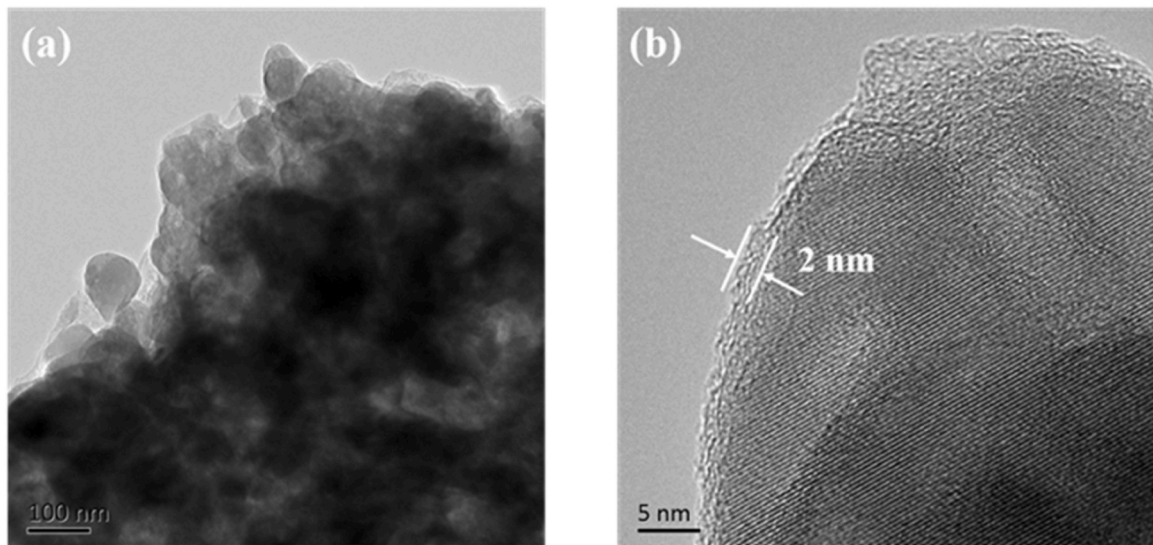


Fig. 3. TEM images of $\text{Li}_{1.05}\text{Fe}_{0.5}\text{Mn}_{0.475}\text{PO}_4/\text{C}$.

Table 1
ICP-OES test results for $\text{Li}_{1.05}\text{Fe}_{0.5}\text{Mn}_{0.475}\text{PO}_4/\text{C}$.

Sample	Mass ratio %			Atomic ratio % Li/Fe/Mn
	Li	Fe	Mn	
$\text{Li}_{1.05}\text{Fe}_{0.5}\text{Mn}_{0.475}\text{PO}_4/\text{C}$	4.54	16.92	15.84	2.151:1:0.952

more active sites for electrochemical reactions, thereby enhancing electrochemical reactivity. Subsequent electrochemical tests further confirm that $\text{Li}_{1.05}\text{Fe}_{0.5}\text{Mn}_{0.475}\text{PO}_4/\text{C}$ exhibits optimal electrochemical performance.

Fig. 5a displays the CV curves of the $\text{Li}_{1.05}\text{Fe}_{0.5}\text{Mn}_{0.5}\text{PO}_4/\text{C}$, $\text{Li}_{1.05}\text{Fe}_{0.475}\text{Mn}_{0.5}\text{PO}_4/\text{C}$ and $\text{Li}_{1.05}\text{Fe}_{0.5}\text{Mn}_{0.475}\text{PO}_4/\text{C}$ electrodes at a scan rate of $0.1 \text{ mV}\cdot\text{s}^{-1}$ under the potential range from 2.0 to 4.5 V vs. Li/Li^+ . The $\text{Li}_{1.05}\text{Fe}_{0.5}\text{Mn}_{0.475}\text{PO}_4/\text{C}$ shows the strongest $\text{Fe}^{3+}/\text{Fe}^{2+}$ and

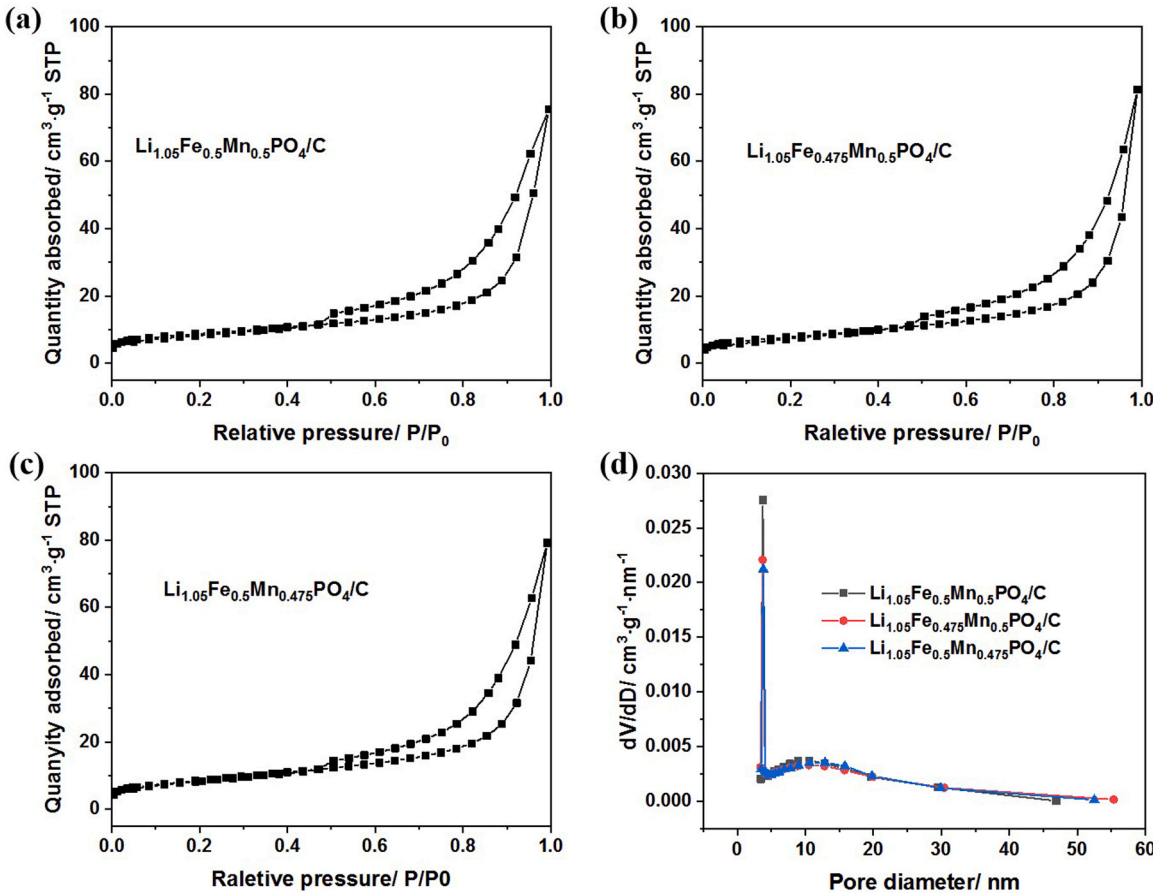


Fig. 4. Nitrogen isotherm sorption curve (a-c) and the pore size distribution (d) of all three samples.

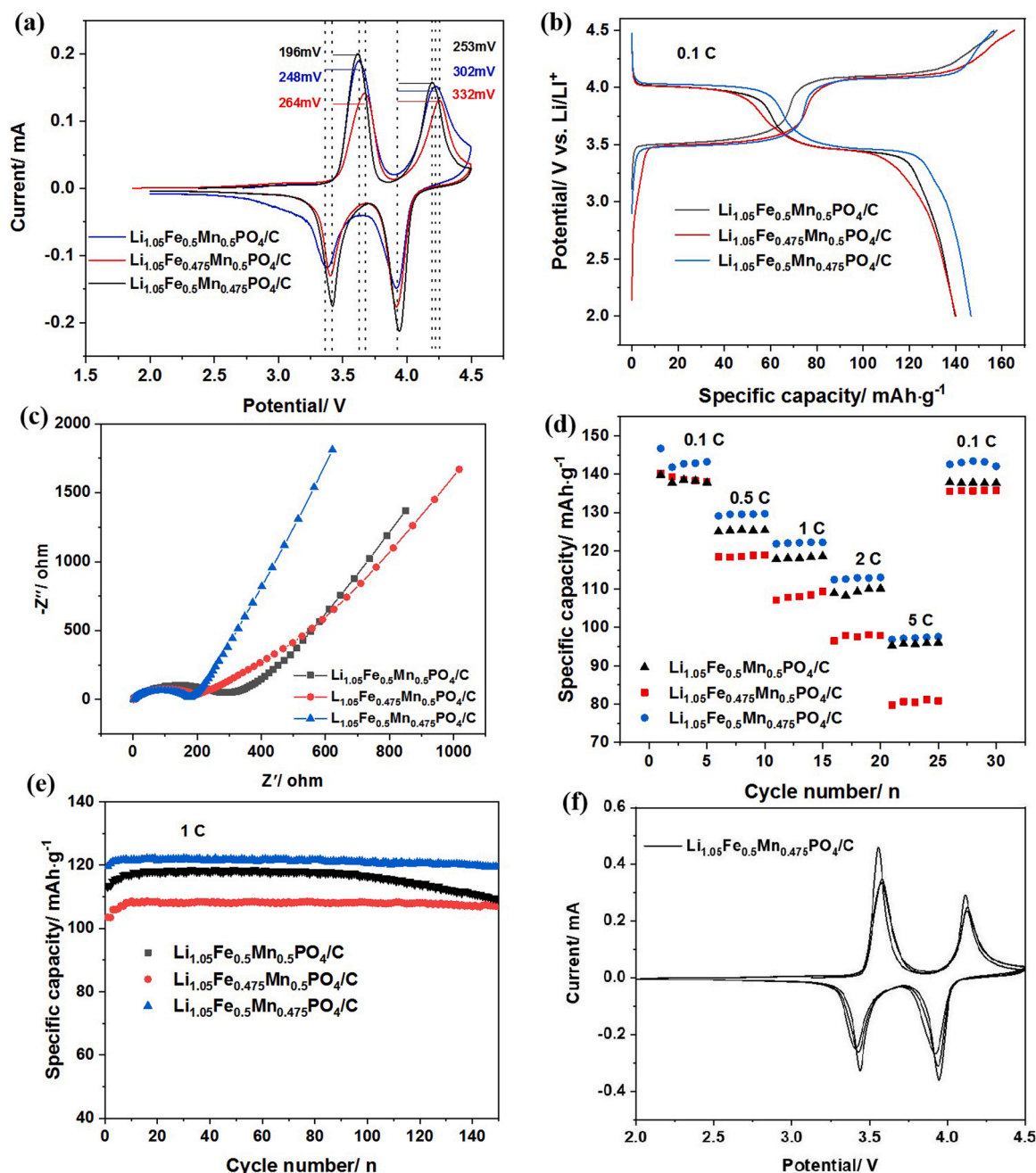


Fig. 5. Comparisons of (a) CVs at a scan rate of 0.1 mV·s⁻¹, (b) charge–discharge curves at 0.1 C, (c) Impedance spectra, (d) the rate performance at different C-rates and (e) cycling performance for three samples, and (f) first three cycles CVs at a scan rate of 0.1 mV·s⁻¹ of $\text{Li}_{1.05}\text{Fe}_{0.5}\text{Mn}_{0.475}\text{PO}_4/\text{C}$.

$\text{Mn}^{3+}/\text{Mn}^{2+}$ redox couples, which are well-distinguished. Furthermore, the smallest voltage difference between the oxidation and reduction peaks suggests that the $\text{Li}_{1.05}\text{Fe}_{0.5}\text{Mn}_{0.475}\text{PO}_4/\text{C}$ sample possesses the

Table 2

Comparisons of the rate performance of the state-of-the-art $\text{LiFe}_{0.5}\text{Mn}_{0.5}\text{PO}_4$ cathode materials.

Sample	Rate performance	Ref.
$\text{LiFe}_{0.5}\text{Mn}_{0.5}\text{PO}_4/\text{C}$	0.1 C: 138, 1 C: 99, 5 C: 80 mAh·g ⁻¹	[11]
	0.1 C: 121, 2 C: 110 mAh·g ⁻¹	[12]
	0.15 C: ~110, 1 C: ~87 mAh·g ⁻¹	[13]
	0.5 C: 133, 1 C: 129, 2 C: 116 mAh·g ⁻¹	[14]
	0.1 C: 130, 0.5 C: 85 mAh·g ⁻¹	[15]
	0.1 C: 116, 1 C: 79, 2 C: 69 mAh·g ⁻¹	[16]
	0.1 C: 143, 1 C: 130, 5 C: 97 mAh·g ⁻¹	This work

fastest kinetics for Li⁺ de-intercalation/intercalation processes among these three samples. And the first three CV tests at a scan rate of 0.1 mV·s⁻¹ are conducted on $\text{Li}_{1.05}\text{Fe}_{0.5}\text{Mn}_{0.475}\text{PO}_4/\text{C}$ (Fig. 5f). The peak current was strongest during the first cycle, but slightly decreased in the second cycle.

The first cycle showed the strongest peak current, while the second cycle slightly decreased. However, in the third cycle, the peak current gradually approached the level of the first cycle, and polarization gradually decreased, which is consistent with the charging and discharging test results. The reason for the increase in polarization is that the Li⁺ diffusion rate and electron transfer rate have not reached a balance, making it impossible to maintain effective charging and discharging currents [10]. As displayed in Fig. 5b, $\text{Li}_{1.05}\text{Fe}_{0.5}\text{Mn}_{0.475}\text{PO}_4/\text{C}$ exhibits a specific discharge capacity of 143.5 mAh·g⁻¹ at 0.1 C rate, with a high coulombic efficiency (CE) of 93.7 % in the first cycle.

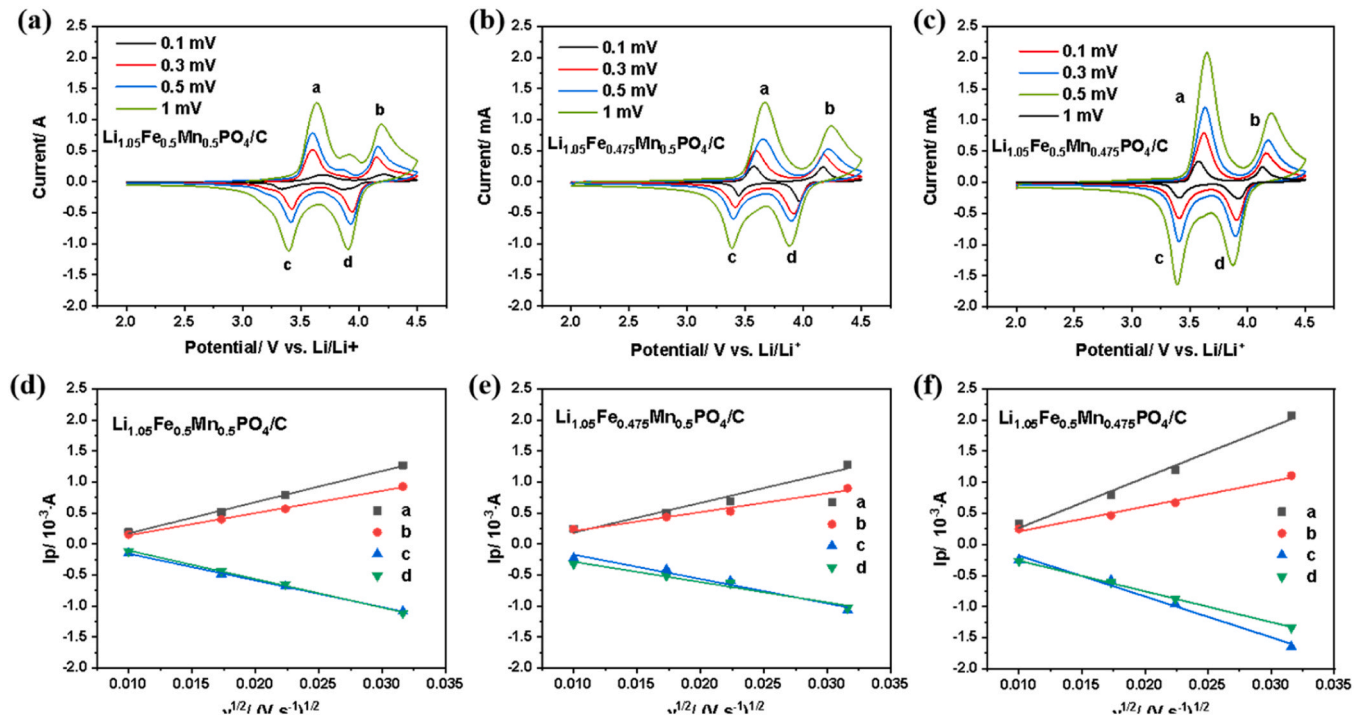


Fig. 6. The CVs at different scan rates and the plots of the peak current (I_p) as a function of the square root of the scanning rate ($v^{1/2}$) for the coin cell made with (a,d) $\text{Li}_{1.05}\text{Fe}_{0.5}\text{Mn}_{0.5}\text{PO}_4/\text{C}$, (b,e) $\text{Li}_{1.05}\text{Fe}_{0.475}\text{Mn}_{0.5}\text{PO}_4/\text{C}$ and (c,d) $\text{Li}_{1.05}\text{Fe}_{0.5}\text{Mn}_{0.475}\text{PO}_4/\text{C}$ composites.

Table 3

Summary of the CV results obtained at different scanning rates and the Li^+ diffusion coefficients (D_{Li^+}) determined for three electrodes.

peak	element	$D_{\text{Li}^+}(\text{cm}^2\cdot\text{s}^{-1})$			
		$\text{Li}_{1.05}\text{Fe}_{0.5}\text{Mn}_{0.5}\text{PO}_4/\text{C}$	$\text{Li}_{1.05}\text{Fe}_{0.475}\text{Mn}_{0.5}\text{PO}_4/\text{C}$	$\text{Li}_{1.05}\text{Fe}_{0.5}\text{Mn}_{0.475}\text{PO}_4/\text{C}$	
Anode	Fe	3.442×10^{-11}	2.751×10^{-11}	7.949×10^{-11}	
	Mn	1.674×10^{-11}	1.106×10^{-11}	1.942×10^{-11}	
Cathode	Fe	2.368×10^{-11}	1.860×10^{-11}	5.203×10^{-11}	
	Mn	2.552×10^{-11}	1.298×10^{-11}	2.966×10^{-11}	

Moreover, it presents a specific discharge capacity of $112.8 \text{ mAh}\cdot\text{g}^{-1}$ at 2.0 C rate. The favorable Li^+ de-intercalation/intercalation behavior of $\text{Li}_{1.05}\text{Fe}_{0.5}\text{Mn}_{0.475}\text{PO}_4/\text{C}$ is also demonstrated by the highest specific capacity, the best rate performance and the lowest charge transfer resistance, as shown in Fig. 5b, c and d, respectively. Comparisons of the rate performance of the state-of-the-art $\text{LiFe}_{0.5}\text{Mn}_{0.5}\text{PO}_4$ cathode materials as shown in Table 2, it is found that $\text{Li}_{1.05}\text{Fe}_{0.5}\text{Mn}_{0.475}\text{PO}_4/\text{C}$ exhibits a superior rate capability. The cycle performance of $\text{Li}_{1.05}\text{Fe}_{0.5}\text{Mn}_{0.475}\text{PO}_4/\text{C}$ at 1 C rate is shown in Fig. 5e, with the initial specific discharge capacities of $119.6 \text{ mAh}\cdot\text{g}^{-1}$. After 150 cycles, it exhibits almost no capacity decay, with the capacity retention of $> 99.9\%$.

A series of CVs recorded from different sweeping rates ($0.1\text{--}1.0 \text{ mV}\cdot\text{s}^{-1}$) between 2.0 and 4.5 V for three samples are shown in Fig. 6a, b and c. It is found that the reduction and oxidation peak potentials in the CV profiles shift toward lower and higher voltages with the increase of the sweeping rate, respectively, with the separation potentials between the anodic and cathodic peaks enhanced in the meantime. Moreover, the peak current (I_p) increases with the raised sweeping rate, exhibiting a well linear relationship with the square root of the scanning rate ($v^{1/2}$), as shown in Figs. 6d, e and f. Based on the Randles Sevcik equation of $I_p = (2.69 \times 10^5) A C_{\text{Li}} D_{\text{Li}}^{1/2} n^{2/3} v^{1/2}$ [17] [where I_p is the peak current value (A), A is the effective working electrode area (cm^2), C_{Li} is the shuttle concentration of Li ions ($\text{mol}\cdot\text{cm}^{-3}$), v is the potential sweeping rate ($\text{V}\cdot\text{s}^{-1}$) and D_{Li} is the diffusion coefficient ($\text{cm}^2\cdot\text{s}^{-1}$)], the calculated Li^+ diffusion coefficients are summarized in Table 3. This relationship indicates that the Li^+ insertion/extraction in

$\text{Li}_{1.05}\text{Fe}_{0.5}\text{Mn}_{0.475}\text{PO}_4/\text{C}$ is a typical diffusion-controlled process, and the diffusion coefficients for the four peaks range from 1.94×10^{-11} to $7.95 \times 10^{-11} \text{ cm}^2\cdot\text{s}^{-1}$. The superior Li^+ diffusion coefficients could be ascribed to the enhanced contact area of $\text{Li}_{1.05}\text{Fe}_{0.5}\text{Mn}_{0.475}\text{PO}_4/\text{C}$ with the electrolyte and the reduced Li^+ diffusion distance, as described and analyzed in the XRD, BET, SEM and TEM sections.

4. Conclusion

In conclusion, this study employed a non-stoichiometric design to ensure the constant total valence of three metal elements, Li, Fe, and Mn, and investigated the modification of LFMP cathode material using the solid-phase method. By exploring various non-stoichiometric approaches, it was observed that particles of $\text{Li}_{1.05}\text{Fe}_{0.5}\text{Mn}_{0.5}\text{PO}_4/\text{C}$ and $\text{Li}_{1.05}\text{Fe}_{0.475}\text{Mn}_{0.5}\text{PO}_4/\text{C}$ exhibited block-like structures with significantly increased dimensions and severe inter-particle crosslinking. XRD analysis revealed elongation of lithium ion one-dimensional diffusion pathways in both cases, accompanied by higher Li_3PO_4 content, leading to increased charge transfer impedance and decreased specific capacity. BET analysis indicated that $\text{Li}_{1.05}\text{Fe}_{0.475}\text{Mn}_{0.5}\text{PO}_4/\text{C}$ possessed the smallest specific surface area ($27.69 \text{ m}^2\cdot\text{g}^{-1}$), resulting in reduced active reaction sites. Electrochemical tests demonstrated excellent discharge specific capacity and cycling performance of $\text{Li}_{1.05}\text{Fe}_{0.5}\text{Mn}_{0.475}\text{PO}_4/\text{C}$. The initial discharge specific capacities at 0.1 C and 5.0 C rates reached 146.7 and $96.8 \text{ mAh}\cdot\text{g}^{-1}$, respectively, while the capacity retention rate remained at 99.8% after 150 cycles at 1.0 C rate. These findings suggest

that the synthesis of $\text{Li}_{1.05}\text{Fe}_{0.5}\text{Mn}_{0.475}\text{PO}_4/\text{C}$ using non-stoichiometric methods facilitates better control over impurity phase content, particle size, and morphology, thus optimizing the electrochemical performance of the material.

Declaration of Competing Interest

The authors declare that they have no known competing financial interests or personal relationships that could have appeared to influence the work reported in this paper.

Acknowledgments

Thanks to Professor Deng Yuanfu from South China University of Technology for his support on this paper. The support received from the Innovation and Entrepreneurship Training Program at South China Agricultural University.

References

- [1] M.K. Devaraju, I. Honma, Hydrothermal and Solvothermal Process Towards Development of LiMPO_4 (M = Fe, Mn) Nanomaterials for Lithium-ion Batteries, *Adv. Energy Mater.* 2(3), 284–297, <https://doi.org/10.1002/aenm.201100642>.
- [2] E.B. Fredj, S. Rousselot, Synthesis and characterization of $\text{LiFe}_{1-x}\text{Mn}_x\text{PO}_4$ ($x = 0.25, 0.50, 0.75$) lithium ion battery cathode synthesized via a melting process, *J. Energy Storage* 27 (2020) 101116, <https://doi.org/10.1016/j.est.2019.101116>.
- [3] D. Kim, S. Lee, Boosting both electronic and ionic conductivities via incorporation of molybdenum for $\text{LiFe}_{0.5}\text{Mn}_{0.5}\text{PO}_4$ cathode in lithium-ion batteries, *J. Alloy. Compd.* (2024) 174396, <https://doi.org/10.1016/j.jallcom.2024.174396>.
- [4] J. Lv, Y. Zheng, Effects of Li^+ enrichment on the structure and microwave dielectric properties of LiMgPO_4 ceramics, *Ceram. Int.* 49 (23) (2023) 37245–37252, <https://doi.org/10.1016/j.ceramint.2023.09.048>.
- [5] H. Zhuang, Y. Bao, Synergistic effect of composite carbon source and simple pre-calcining process on significantly enhanced electrochemical performance of porous $\text{LiFe}_{0.5}\text{Mn}_{0.5}\text{PO}_4/\text{C}$ agglomerations, *Electrochim. Acta* 314 (2019) 102–114, <https://doi.org/10.1016/j.electacta.2019.05.066>.
- [6] X. Zhou, Y. Xie, The enhanced rate performance of $\text{LiFe}_{0.5}\text{Mn}_{0.5}\text{PO}_4/\text{C}$ cathode material via synergistic strategies of surfactant-assisted solid state method and carbon coating, *J. Mater. Chem. A* 3 (2015) 996–1004, <https://doi.org/10.1039/C4TA05431H>.
- [7] Y. Wang, C.Y. Wu, Rational design of a synthetic strategy, carburizing approach and pore-forming pattern to unlock the cycle reversibility and rate capability of microagglomerated $\text{LiMn}_{0.8}\text{Fe}_{0.2}\text{PO}_4$ cathode materials, *J. Mater. Chem. A* 6 (2018) 10395–10403, <https://doi.org/10.1039/C8TA03418D>.
- [8] X. Yan, D.Y. Sun, Enhanced electrochemical performance of $\text{LiMn}_{0.75}\text{Fe}_{0.25}\text{PO}_4$ nanoplates from multiple interface modification by using fluorine-doped carbon coating, *ACS Sustain. Chem. Eng.* 5 (2017) 4637–4644, <https://doi.org/10.1021/acssuschemeng.6b03163>.
- [9] J.F. Qian, M. Zhou, Template-free hydrothermal synthesis of nanoembossed mesoporous LiFePO_4 microspheres for high-performance lithium-ion batteries, *J. Phys. Chem. C* 114 (2010) 3477–3482, <https://doi.org/10.1021/jp912102k>.
- [10] K. Wang, M.Y. Hou, An additional discharge plateau of Mn^{3+} in $\text{LiFe}_{0.5}\text{Mn}_{0.5}\text{PO}_4$ at high current rates, *Electrochem. Commun.* 55 (2015) 6–9, <https://doi.org/10.1016/j.elecom.2015.03.004>.
- [11] K. Saravanan, V. Ramar, P. Balaya, J.J. Vittal, Li ($\text{Mn}_x\text{Fe}_{1-x}$) PO_4/C ($x = 0.5, 0.75$ and 1) nanoplates for lithium storage application, *J. Mater. Chem.* 21 (2011) 14925–14935, <https://doi.org/10.1039/C1JM11541C>.
- [12] S.M. Oh, S.T. Myung, Y.S. Choi, K.H. Oh, Y.K. Sun, Co-precipitation synthesis of micro-sized spherical $\text{LiMn}_{0.5}\text{Fe}_{0.5}\text{PO}_4$ cathode material for lithium batteries, *J. Mater. Chem.* 21 (2011) 19368–19374, <https://doi.org/10.1039/C1JM13889H>.
- [13] Y.J. Zhong, J.T. Li, Z.G. Wu, X.D. Guo, B.H. Zhong, S.G. Sun, $\text{LiMn}_{0.5}\text{Fe}_{0.5}\text{PO}_4$ solid solution materials synthesized by rheological phase reaction and their excellent electrochemical performances as cathode of lithium ion battery, *J. Power Sources* 234 (2013) 217–222, <https://doi.org/10.1016/j.jpowsour.2013.01.184>.
- [14] L. Liu, G. Chen, B. Du, Y.Y. Cui, X. Ke, J. Liu, Z.P. Guo, Z.C. Shi, H.Y. Zhang, S. L. Chou, Nano-sized cathode material $\text{LiFe}_{0.5}\text{Mn}_{0.5}\text{PO}_4/\text{C}$ synthesized via improved sol-gel routine and its magnetic and electrochemical properties, *Electrochim. Acta* 255 (2017) 205–211, <https://doi.org/10.1016/j.electacta.2017.09.165>.
- [15] S. Dhaybi, B. Marsan, $\text{LiFe}_{0.5}\text{Mn}_{0.5}\text{PO}_4/\text{C}$ prepared using a novel colloidal route as a cathode material for lithium batteries, *J. Alloy. Compd.* 737 (2018) 189–196, <https://doi.org/10.1016/j.jallcom.2017.12.064>.
- [16] N.V. Kosova, O.A. Podgornova, A.K. Gutakovskii, Different electrochemical responses of $\text{LiFe}_{0.5}\text{Mn}_{0.5}\text{PO}_4$ prepared by mechanochemical and solvothermal methods, *J. Alloy. Compd.* 742 (2018) 454–465, <https://doi.org/10.1016/j.jallcom.2018.01.242>.
- [17] L.L. Zhang, S. Duan, Novel synthesis of low carbon-coated $\text{Li}_3\text{V}_2(\text{PO}_4)_3$ cathode material for lithium-ion batteries, *J. Alloy. Compd.* 570 (2013) 61–64, <https://doi.org/10.1016/j.jallcom.2013.03.189>.

检索证明

根据委托人提供的论文材料，委托人华南农业大学基础实验与实践训练中心 庄慧 1 篇论文收录情况如下表。

序号	论文名称	发表刊物及发表的年月卷期/页码等	作者排名	论文等级	作者文中单位	收录情况	影响因子	中科院大类分区
1	Preparation of lithium ferromanganese phosphate by non-stoichiometric strategy	INTERNATIONAL JOURNAL OF ELECTROCHEMICAL SCIENCE 出版年：2024 出版日期：AUG 卷期：19 8 页码： 文献号：100636 文献类型：Article	第一及通讯	B类	Experimental Basis and Practical Training Center, South China Agricultural University	SCI	IF2-year=2.4 IF5-year=1.8 (2024)	化学 4区 Top 期刊：否 (2023)

说明：论文等级和中科院大类分区按《华南农业大学学术论文评价方案（试行）》划分。

报告免责声明：如未盖章，报告无效

